2013

Model Reference Adaptive System-Based Speed Estimators for Sensorless Control of Interior Permanent Magnet Synchronous Machines

Yue Zhao
University of Nebraska-Lincoln, yue.zhao@huskers.unl.edu

Wei Qiao
University of Nebraska–Lincoln, wqiao@engr.unl.edu

Long Wu
John Deere Electronic Solutions, WuLong@JohnDeere.com

Transportation Electrification Conference and Expo (ITEC), 2013 IEEE
Year: 2013
Pages: 1 - 6, DOI: 10.1109/ITEC.2013.6574514

Model Reference Adaptive System-Based Speed Estimators for Sensorless Control of Interior Permanent Magnet Synchronous Machines

Yue Zhao, Wei Qiao
Department of Electrical Engineering
University of Nebraska-Lincoln
Lincoln, NE 68588-0511 USA
yue.zhao@huskers.unl.edu; wqiao@engr.unl.edu

Long Wu
John Deere Electronic Solutions
4101 19th Avenue North
Fargo, ND 58102 USA
WuLong@JohnDeere.com

***Abstract*--In this work, speed estimators are designed based on a model reference adaptive system (MRAS) for sensorless control of interior permanent magnet synchronous machines (IPMSMs). To provide better filtering performance and reduce the noise contents in the estimated speed, an adaptive line enhancer is proposed to work with a sliding-mode observer to provide an improved reference model for speed estimation. In addition, a heterodyning speed adaption scheme is proposed to replace the conventional speed adaption mechanism. The proposed MRAS-based speed estimator has two different operating modes, which are suitable for generator- and motor-type applications, respectively. The effectiveness of the proposed speed estimators are verified by simulation using real-word vehicle data logged from a test vehicle. Furthermore, experimental results on a test stand for a heavy-duty IPMSM are also provided.**

***Keywords*—Interior permanent magnet synchronous machine (IPMSM), model reference adaptive system (MRAS), sensorless control, speed estimator.**

I. INTRODUCTION

Interior permanent magnet synchronous machines (IPMSMs) are widely used in electric and hybrid electric vehicle systems owing to their distinctive advantages, such as high efficiency, high power density and wide constant power region. To achieve high-performance vector control for IPMSMs, accurate rotor position information is indispensable, which, in conventional IPMSM drive systems, is usually obtained by electromechanical position sensors, e.g., optical encoders, resolvers, and hall-effect sensors. To reduce the cost and improve the reliability of the drive system, much research effort has gone into the development of position/speed sensorless drives that have comparable dynamic performance to sensor-based drives during the last decades.

In sensorless IPMSM drive systems, especially for medium- and high-speed applications, rotor position and speed can be estimated by using sensed machine voltages and currents. Several full-order observers [1], [2] have been proposed for simultaneous rotor position and speed estimation. However, the full-order observers are usually complicated, which were built on high-order, e.g., fourth-order equations. In addition, it is difficult to guarantee the convergence of both speed and position estimation simultaneously in fast varying speed/torque conditions. To simplified the algorithm and improve the transient tracking performance, several reduced-order observers, such as disturbance observers [3] and sliding-mode observers (SMO) [4], [5], have been proposed, and were verified to be effective in sensorless IPMSM drive systems. By using second-order equations, the observers can effectively estimate one state of interest, i.e., either rotor position or speed. Then, based on the relationship between speed and position, the other state can be calculated. Therefore, there are two major types of reduced-order observers, which are illustrated in Fig. 1. In practical applications, due to the cascade structure, the performance of position and speed estimations may not be acceptable during large load and machine parameter variations.

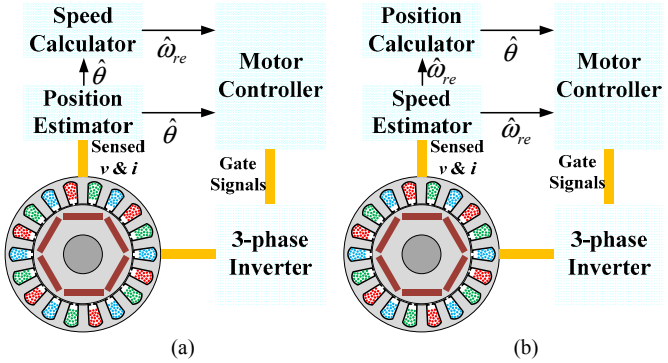

Fig. 1. Illustration of the reduced-order observer-based rotor position/speed estimators based on (a) position and (b) speed estimation.

In [5], a SMO based on the machine model in the $\alpha\beta$ stationary reference frame was proposed. The SMO generates a switching output $Z_{\alpha\beta}$, which contains not only the information of the back electromotive force (EMF), but also high-order harmonics and heavy noise. Therefore, a low-pass filter was utilized to extract the estimated EMF from $Z_{\alpha\beta}$, and the filtered estimated EMF was further used to calculate the rotor position through a position extraction subsystem, e.g., a trigonometric method or an angle tracking observer (ATO). Finally, the rotor speed is calculated by using a phase-locked loop (PLL). As shown in Fig. 1(a), several inherent

978-1-4799-0148-7/13/$31.00 ©2013 IEEE

drawbacks exist in this position/speed estimation system. First of all, since the position estimator and the speed calculator are sequentially connected, there is neither a feedback nor other adjustment schemes, which results in error propagation. For instance, if the back EMF filter has improper parameters, the following position and speed calculation will be affected. What's worse, since the speed calculator is the last block, it will be affected by the performance of all the subsystems prior to it. Secondly, the position estimation is sensitive to load conditions. Since the speed is calculated from the estimated position, the speed estimation is also sensitive to load variations. A different example was presented in [3], in which a disturbance observer was proposed based on the machine model in the estimated $\gamma\delta$ rotating reference frame, in which the rotor speed was first estimated. Then, based on the estimated speed, an integrator was used to calculate the rotor position. The structure of such position/speed estimation is illustrated in Fig. 1(b), in which the speed estimator and position calculator are also connected in series, resulting in similar drawbacks as those of the system in Fig. 1(a).

To solve the problems of the estimators in Fig. 1, the most effective solution is to decouple the speed and position estimation, i.e., estimating the two states independently. In this paper, an SMO [6] is designed to estimate the extended EMF (EEMF) of IPMSMs. Based on the estimated EEMF, the rotor position and speed are estimated separately. A model reference adaptive system (MRAS)-based speed estimator is proposed to estimate the rotor speed. An adaptive line enhancer (ALE) is proposed to do EEMF filtering without introducing any phase delay between the original and filtered EEMF. With the proposed ALE, the SMO becomes an improved reference model in the MARS. In addition, a heterodyning speed adaption mechanism is proposed. The proposed MRAS speed estimator has two different operating modes, which can be utilized for different applications in vehicles, such as traction motors and generators. The proposed MRAS-based speed estimator is validated by simulation results using real-world vehicle data and experimental results on a 150 kW sensorless IPMSM drive used for heavy-duty, off-road, hybrid electric vehicles.

II. Conventional MRAS-based Speed Estimator for IPMSMs

The MRAS [7]-[10] is an effective scheme for speed estimation in motor drives, e.g., induction motors [9], brushless DC motors [10], and PMSMs [7]. In a MRAS, an adjustable model and a reference model are connected in parallel. A typical structure of the conventional MRAS-based speed estimator is shown in Fig. 2. In this paper, the EEMF is estimated by using an SMO [6], which is a good candidate of the reference model. Then, an adjustable model should be designed, whose output is expected to converge to the output of the reference model with a proper adaption mechanism. Since the estimated speed is one of the internal states of the adjustable model, if the output of the adjustable model well tracks the output of the reference model, the internal states of the two models should be identical. From this point of view the adjustable model is a kind of adaptive observer. If the adaption mechanism is well designed, the error between the reference model and adjustable model should be close to zero. Therefore, accurate speed estimation can be achieved.

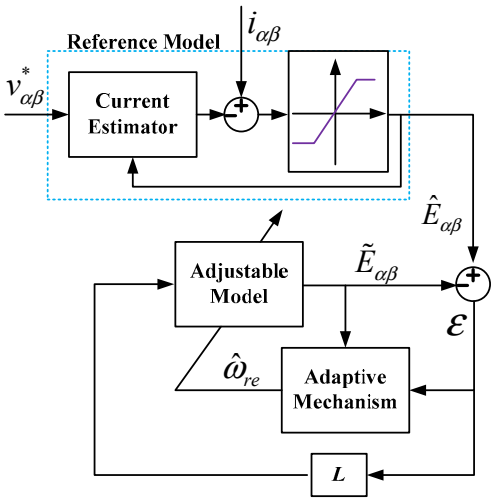

Fig. 2. Schematic of the conventional MRAS-based speed estimator.

The design of the adjustable model is originated from the EEMF model of an IPMSM, which can be expressed as:

$$\begin{bmatrix} v_\alpha \\ v_\beta \end{bmatrix} = \begin{bmatrix} R + pL_d & \omega_{re}(L_d - L_q) \\ \omega_{re}(L_q - L_d) & R + pL_d \end{bmatrix} \begin{bmatrix} i_\alpha \\ i_\beta \end{bmatrix} + \begin{bmatrix} E_\alpha \\ E_\beta \end{bmatrix} \quad (1)$$

where p is the derivative operator; v_α and v_β are the stator voltages; i_α and i_β are the stator currents; ω_{re} is the electrical rotor speed; R is the stator resistance; L_d and L_q are the d-axis and q-axis inductances, respectively; and the EEMF components are defined as:

$$\begin{bmatrix} E_\alpha \\ E_\beta \end{bmatrix} = \left[(L_d - L_q)(\omega_{re} i_d - p i_q) + \omega_{re} \psi_m \right] \begin{bmatrix} -\sin\theta \\ \cos\theta \end{bmatrix}.$$

By using the properly designed SMO, the estimated EEMF, $\hat{E}_{\alpha\beta} = [\hat{E}_\alpha,\ \hat{E}_\beta]^{\mathrm{T}}$, can be obtained. If the rotor speed changes slowly, i.e., $d\omega_{re}/dt \approx 0$ (This is true especially when considering fast changing rotor position in the medium- and high-speed region), the derivative of the estimated EEMF components can be calculated as:

$$\begin{cases} \dot{\hat{E}}_\alpha = -\omega_{re} \hat{E}_\beta \\ \dot{\hat{E}}_\beta = \omega_{re} \hat{E}_\alpha \end{cases} \quad (2)$$

The adjustable model can be designed following (2) as:

$$\begin{bmatrix} \dot{\tilde{E}}_\alpha \\ \dot{\tilde{E}}_\beta \end{bmatrix} = \hat{\omega}_{re} \underbrace{\begin{bmatrix} 0 & -1 \\ 1 & 0 \end{bmatrix}}_{J} \cdot \begin{bmatrix} \tilde{E}_\alpha \\ \tilde{E}_\beta \end{bmatrix} + \underbrace{\begin{bmatrix} L_{11} & L_{12} \\ L_{21} & L_{22} \end{bmatrix}}_{\mathrm{L}} \cdot \begin{bmatrix} \hat{E}_\alpha - \tilde{E}_\alpha \\ \hat{E}_\beta - \tilde{E}_\beta \end{bmatrix} \quad (3)$$

where $\tilde{E}_{\alpha\beta} = [\tilde{E}_\alpha, \tilde{E}_\beta]^{\mathrm{T}}$ is the output of the adjustable model, which is still an estimation of the EEMF; $\hat{\omega}_{re}$ is the

estimated electrical rotor speed, which is the output of the adaptive mechanism. **L** is the MRAS gain matrix, which can be configured by using linear observer design techniques, e.g., pole assignments [8]. In practical applications, the off-diagonal elements, L_{21} and L_{12}, can be set as zero [7] to simplify the design procedure.

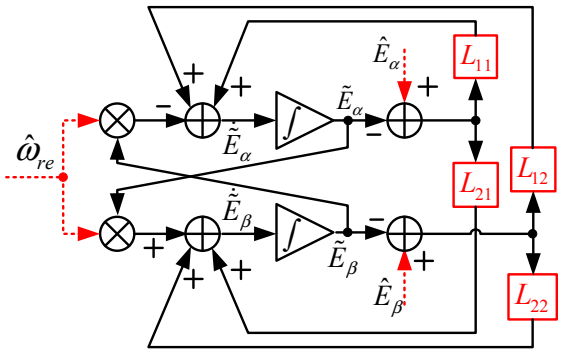

Fig. 3. Block diagram of a typical adjustable model.

Based on the outputs of the adjustable model and the reference model, the rotor speed can be estimated by using a proportional-integral (PI) speed regulator as:

$$\hat{\omega}_e = \left(k_p + \frac{k_i}{s}\right)\left[\left(\hat{E}_{\alpha\beta} - \tilde{E}_{\alpha\beta}\right)^T \cdot J \cdot \tilde{E}_{\alpha\beta}\right] \tag{4}$$

III. Proposed New MRAS-Based Speed Estimator

In the previous section, the conventional MRAS using an SMO as the reference model has been discussed. However, when applying this method to a practical drive system, the SMO does not seem to be an effective reference model. Firstly, this is due to the inherent nonlinearity of the switching function, e.g., a sign function or saturation function, used in the SMO. This nonlinear effect will bring heavy noisy contents in the output of the SMO. Secondly, the EEMF of an IPMSM is both torque- and speed-dependent. Rewrite the expression of the EEMF defined in (1):

$$\begin{bmatrix} E_\alpha(t) \\ E_\beta(t) \end{bmatrix} = \eta(t) \cdot \begin{bmatrix} -\sin\left[\omega_{re}(t) \cdot t + \theta_0\right] \\ \cos\left[\omega_{re}(t) \cdot t + \theta_0\right] \end{bmatrix} \tag{5}$$

where θ_0 is the initial rotor position. The magnitude of the EEMF, $\eta(t)$, is time-variant and depends on the magnitudes of currents and speed. Under fast varying load conditions, e.g., continuous torque jittering, the current derivative term, pi_q, could be a large and varying component, which results in a larger variation in $\eta(t)$. In addition, when the torque is not constant, the rotor speed, ω_{re}, will also be affected.

Considering these two issues, an ALE is designed as a filter for the estimated EEMF. By using the ALE, the noise content in the EEMF can be effectively filtered out. The resulting SMO with the ALE is an improved reference model. In addition, (4) is replaced by the proposed heterodyning speed adaption mechanism, which consumes less computational source than (4). A standard method to determine the PI gains is transfer function-based pole assignment.

A. Adaptive Line Enhancer

Consider a noisy input signal, which consists of a few desired sinusoidal components. When the frequencies of the sinusoidal components presented in the noisy signal are known, a fixed filter will be sufficient. However, when the sine-wave frequencies are unknown or time-varying, e.g., the EEMF components in (5), an adaptive solution, e.g., an ALE [12], has to be adopted.

More specifically, consider that a noisy signal contains single sinusoidal component. Suppose that the input of the ALE, $x(n)$, can be modeled as:

$$x(n) = a\sin(\omega_0 n + \theta) + v(n) \tag{5}$$

where ω_0 is the frequency of the desired sinusoidal signal, and $v(n)$ is the noise, which is not necessary to be white. However, the samples of the noise term, which are more than M sampling intervals apart, are uncorrelated with each other. In this case, the ALE is an M-step-ahead predictor. Fig. 4 depicts the block diagram of an ALE, which can only predict the sinusoidal component in $x(n)$, while filtering out the noise component. When the filter, $W(z)$, is adapted to minimize the output mean-square error (MSE), the ALE will be a filter tuned to sinusoidal component. The output of the filter, $y(n)$, will be an approximation of the sinusoidal component. In the case that $x(n)$ has multiple frequency components, the filtering mechanism is the same. Consider (5) again, if current and speed are time-variant, the EEMF components can be modeled as sums of all the sinusoidal components with different frequencies as follows:

$$\begin{bmatrix} E_\alpha(t) \\ E_\beta(t) \end{bmatrix} = \sum_{i=0}^{L} \begin{Bmatrix} -\sin\left[\omega_i t + \theta_i(t)\right] + v_i(t) \\ \cos\left[\omega_i t + \theta_i(t)\right] + v_i(t) \end{Bmatrix} \tag{6}$$

where ω_i is the frequency of the i^{th} component; $\theta_i(t)$ and $v_i(t)$ are the corresponding time-variant phase angle and noise, respectively; L the number of the sinusoidal components. The number of the filter taps, K, should be greater than L, and the tap weight matrix, $\mathbf{w} = [w_0, w_1, \cdots, w_K]$, can be calculated online by using the celebrated least-mean-square (LMS) algorithm:

$$\mathbf{w}(n+1) = \mathbf{w}(n) + 2\mu e(n)x(n) \tag{7}$$

where μ is the step size for **w** adaption. The simulation result for a simple case study is shown in Fig. 5.

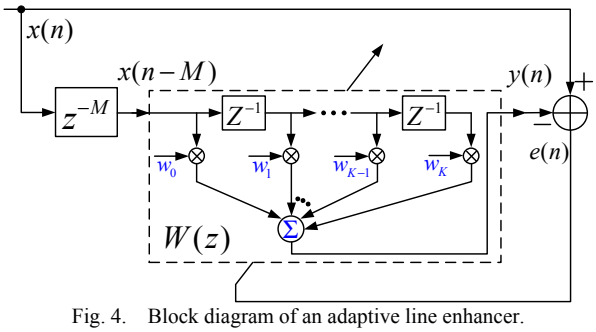

Fig. 4. Block diagram of an adaptive line enhancer.

The desired signal consists of three sinusoidal components with the frequencies of 10 Hz, 20 Hz and 30 Hz, respectively. The power of the noise is equal to that of the desired signal. The sampling frequency is 1 kHz. As the result shows, the

ALE effectively filters out the noise contents without phase shift and magnitude decrease. The output of the ALE converges to the desired signal within 30 samples.

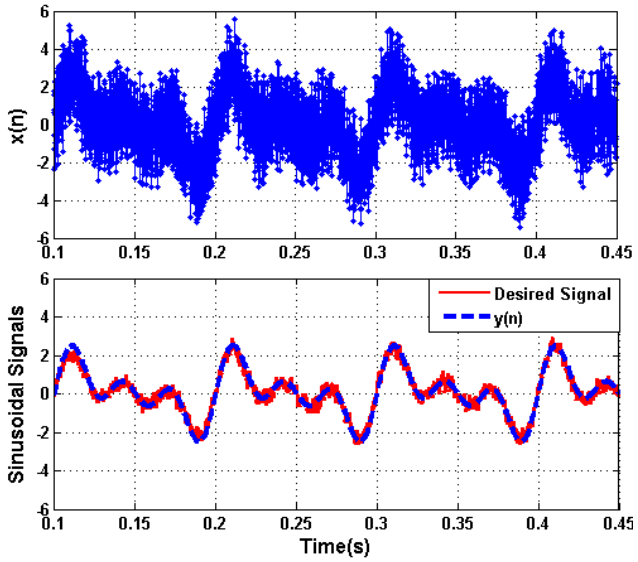

Fig. 5. Simulation result of ALE with artificial data input.

B. Heterodyning Speed Adaption Mechanism

In addition to the ALE, this paper proposes to use heterodyne to replace (4) as the adaptive mechanism. By using the two estimated EEMFs $\hat{E}_{\alpha\beta}$ and $\tilde{E}_{\alpha\beta}$ in the MRAS, the heterodyning speed adaption scheme can be expressed as:

$$\hat{\omega}_{re} = \left(k_p + \frac{k_i}{s}\right)\left(\hat{E}^n_\beta \tilde{E}^n_\alpha - \hat{E}^n_\beta \tilde{E}^n_\alpha\right) \tag{8}$$

where the superscript n stands for normalized values. Let $\hat{\theta}$ and $\tilde{\theta}$ represent the positions obtained from $\hat{E}_{\alpha\beta}$ and $\tilde{E}_{\alpha\beta}$, respectively and define

$$\hat{E}^n_{\alpha\beta} = \begin{bmatrix} -\sin\hat{\theta} & \cos\hat{\theta} \end{bmatrix}^T \quad \text{and} \quad \tilde{E}^n_{\alpha\beta} = \begin{bmatrix} -\sin\tilde{\theta} & \cos\tilde{\theta} \end{bmatrix}^T \tag{9}$$

Substituting (9) into (8) yields:

$$\begin{aligned} \hat{\omega}_{re} = s\tilde{\theta} &= \left(k_p + \frac{k_i}{s}\right)\left(-\cos\hat{\theta}\sin\tilde{\theta} + \sin\hat{\theta}\cos\tilde{\theta}\right) \\ &= \left(k_p + \frac{k_i}{s}\right)\sin\left(\hat{\theta} - \tilde{\theta}\right) \xrightarrow{\Delta\theta = \hat{\theta} - \tilde{\theta} \approx 0} \approx \left(k_p + \frac{k_i}{s}\right)\Delta\theta \end{aligned} \tag{10}$$

Then the transfer function can be expressed as:

$$\frac{\tilde{\theta}}{\hat{\theta}} = \frac{k_p s + k_i}{s^2 + k_p s + k_i} \tag{11}$$

Equation (11) is the second order and has one zero. The dynamic behavior of (11) depends on the PI gains, which can be determined by properly placing the poles of the characteristic polynomial.

C. Overall Speed Estimator

By using the SMO with the ALE, the proposed adaptive mechanism, and the adjustable model, an integrated MRAS-based speed estimator can be obtained. The overall block diagram of the proposed speed estimator is shown in Fig. 6.

The proposed speed estimator has two operating modes, which are suitable for different applications. For Mode I, the error feedback to the adjustable model is the difference between the normalized $\hat{E}_{\alpha\beta}$ and $\tilde{E}_{\alpha\beta}$. Due to the filtering effect of the ALE, the dynamic response of speed tracking will be slightly affected. However, the estimated speed will have less noise contents, which results in a smooth speed profile. Therefore, Mode I is suitable for generator applications, in which the generator is normally operated in the torque control mode and the shaft speed is maintained by a prime mover machine. Therefore, the sensorless control performance is not sensitive to the estimated speed for generator applications.

For Mode II, the error feedback to the adjustable model is the difference between the normalized $Z_{\alpha\beta}$ and $\tilde{E}_{\alpha\beta}$. Since $Z_{\alpha\beta}$ is the unfiltered output of the SMO, sending the information of $Z_{\alpha\beta}$ back to the adjustable model will actively force the output of the adjustable model to approach the unfiltered EEMF estimated from the SMO. This scheme will mitigate the misadjustment due to the ALE during abrupt speed changes and improve the dynamic response of the speed tracking. However, the estimated speed will have relatively larger noise contents, compared to that in Mode I, which results in small speed oscillations. Therefore, Mode II is suitable for the motor applications in electric vehicles, in which the sensorless drive requires accurate speed information without any delay, especially in the speed control mode.

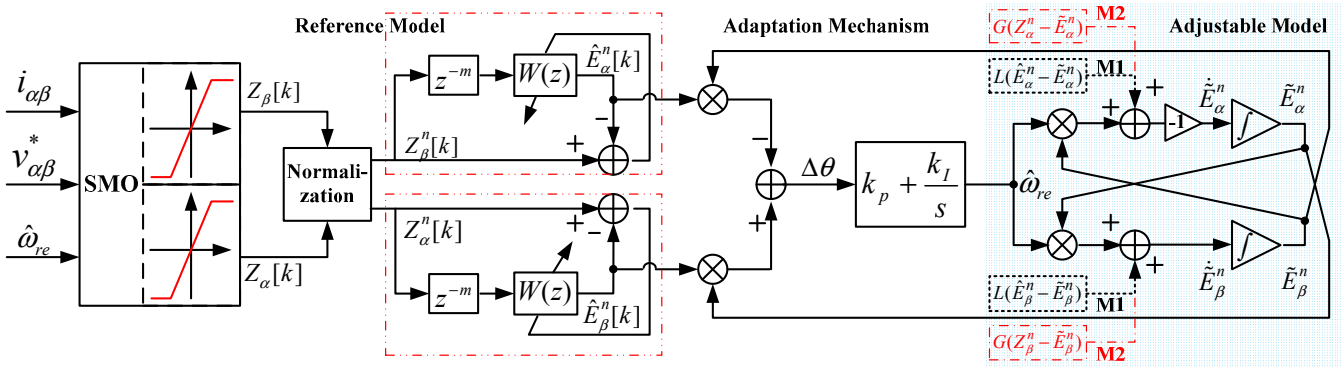

Fig. 6. Block diagram of the proposed MRAS-based speed estimator.

IV. Simulation Results

To verify the performance of the proposed MRAS-based speed estimator, real-world vehicle data are used for simulation studies. The vehicle data are logged from an IPMSM generator on a test vehicle. Fig. 7 depicts the system states, including the generator torque, speed, and DC-bus voltage, during one typical operating cycle. In the simulation, the IPMSM is operated in the torque control mode, and the generator torque profile shown in Fig. 7 is used as the torque command. When the torque has a higher slew-rate change, e.g., around 104 s, an obvious abrupt speed dip is observed correspondingly, which is a critical period for performance evaluation of the proposed speed estimators.

The corresponding simulation results of the estimated speeds obtained from the proposed speed estimator are shown in Fig. 8, which includes the speed command, the estimated speeds obtained from the estimated position using a moving average (MA) filter and the speeds obtained from the proposed MRAS speed estimator in both operating modes. During the large speed transient around the 104th second, the speeds estimated by the MA and the proposed MRAS in Mode I can well track the desired value. However, both of the estimated speeds have obvious delays and relatively large oscillations caused by the load transition. Compared to the MA, the magnitude of the speed oscillation obtained from the MRAS in Mode I is much smaller. Compared to the MA and the MRAS Mode I, the magnitude of the speed oscillation obtained from the MRAS in Mode II at around the 104th second can be neglected. The error between the speed command and the speed estimated by using the MRAS in Mode II is also shown in Fig. 8, which shows that the speed error is always smaller than 1% (using 5,000 RPM as the base).

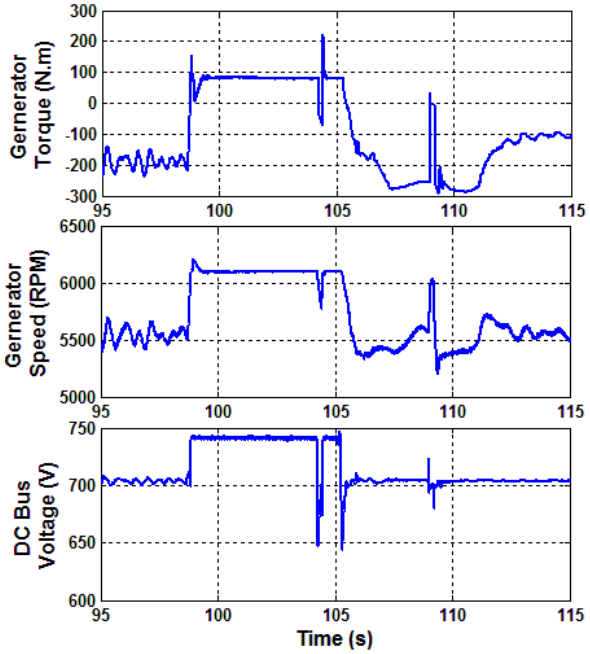

Fig. 7. Real-world vehicle data profiles used for simulation.

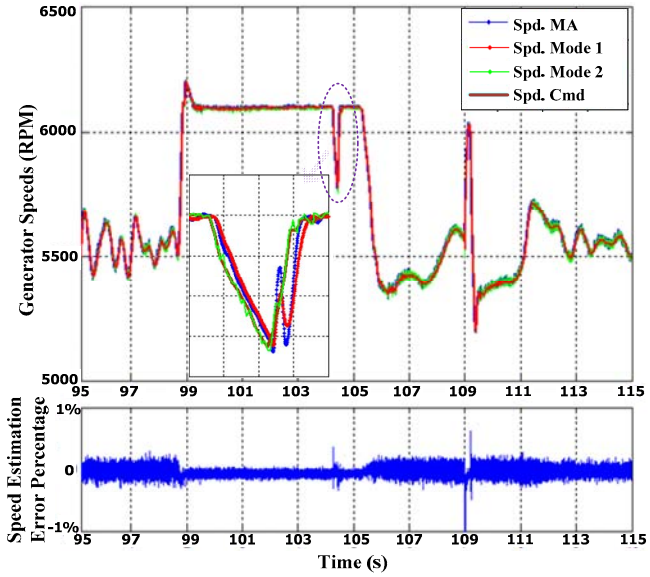

Fig. 8. Speed estimation performance using the proposed speed estimator.

V. Experimental Results

A. Experimental Test Stand Description

A test stand is designed to verify the effectiveness of the proposed MRAS-based speed estimators. In the test stand, a prime mover machine and an IPMSM are connected back to back sharing a common 700-V DC bus connected to a power supply. The prime mover machine maintains the shaft speed while the IPMSM works as a generator in the torque control mode. The schematic of the test stand is shown in Fig. 9. The specification of the test IPMSM is listed in Table. I.

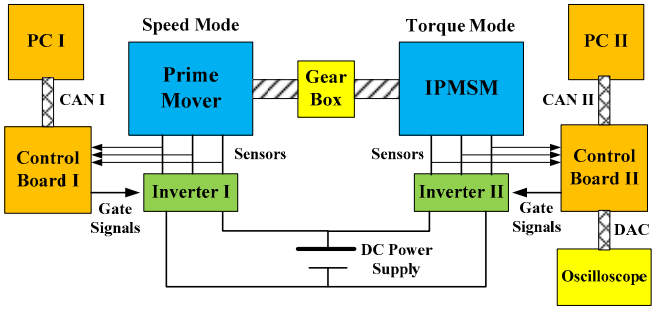

Fig. 9. Schematic of the test stand for the IPMSM.

TABLE I
Specification of the Test IPMSM

Nominal power	150 kW	Stator resistance	0.01 Ω
Maxium torque	300 Nm	Base speed	5,000 RPM
Current	400 A	Pole-pairs number	4
Average L_d	0.17 mH	Average L_q	0.53 mH

B. Results under Complete Torque Reversal

Complete torque reversals, i.e., reversing the torque from the rated motoring torque to the rated braking toque, are used to mimic a large load transient in Fig. 7. The performance of the conventional MRAS and the proposed MRAS Mode II is shown in Fig. 10(a) and (b), respectively. Because of fast torque reversals, the rotor speed has sudden changes, e.g.,

around 500 RPM speed drop in Fig. 10(a) and 500 RPM speed increase in Fig. 10(b). Both of the methods can track the speed changes. However, the speed estimated form the conventional MRAS has unwanted oscillations. However, no obvious oscillation is observed in the speed estimated from the proposed MRAS Mode II. As the plots of speed estimation errors show, for the proposed MRAS Mode II, the speed estimation error is smaller than 1% during steady state and smaller than 2% during large load transient.

VI. Conclusion

A robust speed estimator based on an MRAS structure has been proposed for sensorless IPMSM drives. To provide a better noise cancellation effect for the EEMF, an ALE has been proposed to work with the SMO, leading to an improved reference model. In addition, a heterodyning speed adaption scheme has been proposed to replace the conventional speed adaption mechanism. The proposed speed estimator has two operating modes, which are suitable for IPMSM generator and motor applications, respectively. The effectiveness of the proposed speed estimators have been verified by both simulation and experimental results.

Acknowledgment

This work was supported in part by the National Science Foundation under grant ECCS-0901218.

References

[1] S. Po-ngam and S. Sangwongwanich, "Stability and dynamic performance improvement of adaptive full-order observers for sensorless PMSM Drive," *IEEE Trans. Power Electronics,* vol. 27, no. 2, pp. 588-600, Feb. 2012.

[2] Z. Xu and M. F. Rahman, "An adaptive sliding stator flux observer for a direct-torque-controlled IPM synchronous motor drive," *IEEE Trans. Industrial Electronics*, vol. 54, no. 5, pp. 2398-2406, Oct. 2007.

[3] S. Morimoto, K. Kawamoto, M. Sanada, and Y. Takeda, "Sensorless control strategy for salient-pole PMSM based on extended EMF in rotating reference frame," *IEEE Trans. Industry Applications,* vol. 38, no. 4, pp. 1054-1061, Jul/Aug 2002.

[4] Z. Chen, M. Tomita, S. Doki, and S. Okuma, "An extended electromotive force model for sensorless control of interior permanent-magnet synchronous motors," *IEEE Trans. Industrial Electronics*, vol. 50, no. 2, pp. 288- 295, Apr 2003.

[5] S. Chi, Z. Zhang, and L. Xu, "Sliding-mode sensorless control of direct-drive PM synchronous motors for washing machine applications," *IEEE Trans. Industry Applications*, vol. 45, no. 2, pp. 582-590, Mar.-Apr. 2009.

[6] Y. Zhao, W. Qiao, and L. Wu, "An adaptive quasi-sliding-mode rotor position observer-based sensorless control for IPMSMs," IEEE Trans. Power Electronics, in press.

[7] C. Li and M. Elbuluk, "A sliding mode observer for sensorless control of permanent magnet synchronous motors," in Proc. IEEE IAS Annual Meeting, Oct. 2001, vol. 2, pp.1273-1278.

[8] C. Schauder, "Adaptive speed identification for vector control of induction motors without rotational transducers," in *Proc. IEEE IAS Annual Meeting,* Oct. 1989, vol. 1, pp.493-499.

[9] F. Z. Peng and T. Fukao, "Robust speed identification for speed sensorless vector control of induction motors," *IEEE Trans. Industry Applications*, vol. 30, no. 5, pp. 1234–1240, Sep.-Oct. 1994.

[10] M. Tomita, T. Senjyu, S. Doki, and S. Okuma, "New sensorless control for brushless DC motors using disturbance observers and adaptive velocity estimations," *IEEE Trans. Industrial Electronics*, vol. 45, no. 2, pp. 274-282, Apr 1998.

[11] W. Qiao, X. Yang, and X. Gong, "Wind speed and rotor position sensorless control for direct-drive PMG wind turbines," *IEEE Trans. Industry Applications*, vol. 48, no. 1, pp. 3-11, Jan.-Feb. 2012.

[12] B. Farhang-Boroujeny, *Adaptive Filters Theory and Applications*, 1st Ed, Wiley, 1999.

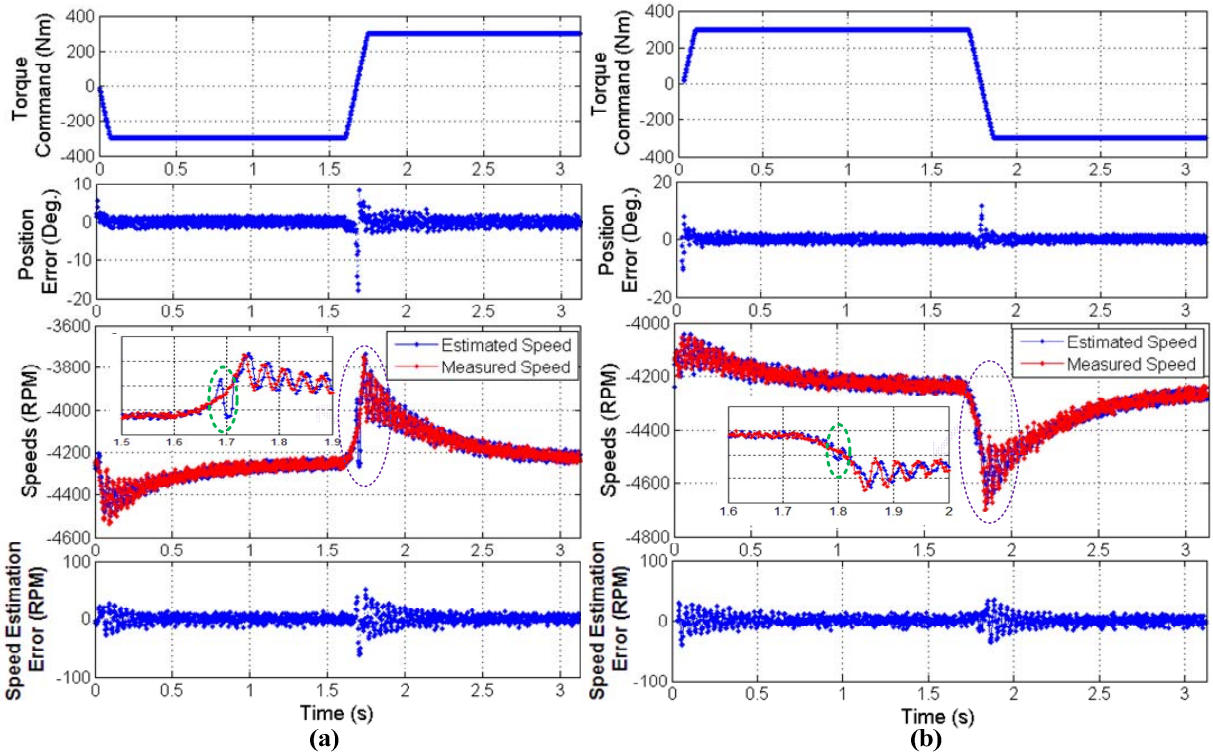

Fig. 10. Experimental results during complete torque reversals: (a) conventional MRAS and (b) proposed MRAS Mode II.